

This is the pre-peer reviewed version of the article. The final, peer-reviewed version can be found at <https://doi.org/10.1002/cctc.202301113>.

# Artificial Metalloenzymes for Atroposelective Metathesis

Tobias Vornholt<sup>+1,2</sup>, Zlatko Jončev<sup>+2,3</sup>, Valerio Sabatino<sup>2,4</sup>, Sven Panke<sup>1,2</sup>, Thomas R. Ward<sup>\*2,4</sup>, Christof Sparr<sup>\*2,3</sup>, Markus Jeschek<sup>\*1,5</sup>

<sup>1</sup>Department of Biosystems Science and Engineering, ETH Zurich, Mattenstrasse 26, 4058 Basel, Switzerland

<sup>2</sup>National Centre of Competence in Research (NCCR) Molecular Systems Engineering, Switzerland; Web: [www.nccr-mse.ch](http://www.nccr-mse.ch)

<sup>3</sup>Department of Chemistry, University of Basel, St. Johannis-Ring 19, 4056 Basel, Switzerland

<sup>4</sup>Department of Chemistry, University of Basel, Mattenstrasse 22, 4058 Basel, Switzerland

<sup>5</sup>Institute of Microbiology, University of Regensburg, Universitätsstraße 31, 93053 Regensburg, Germany

+ These authors contributed equally to this work.

\* Corresponding authors

## Abstract

Atropisomers – separable conformers that arise from restricted single-bond rotation – are frequently encountered in medicinal chemistry. Atroposelective synthesis can therefore be critical for preparing such compounds with a desired configuration. This is, however, often challenging using small-molecule catalysts. Herein, we present an alternative, biocatalytic strategy to achieve atroposelective synthesis relying on artificial metalloenzymes (ArMs). Based on the biotin-streptavidin technology, we constructed ruthenium-bearing ArMs capable of producing atropisomeric binaphthalene compounds through ring-closing metathesis in aqueous media. Further, we show that atroposelectivity can be fine-tuned by engineering two close-lying amino acid residues within the streptavidin host protein. The resulting ArMs promote product formation with enantiomeric ratios of up to 81:19, while corresponding small-molecule catalysts to achieve atroposelectivity by metathesis under aqueous reaction conditions are yet unknown. This study represents the first demonstration that stereoselective metathesis can be achieved by an artificial enzyme.

## Introduction

Atropisomerism occurs when two parts of a molecule cannot rotate freely about a single bond due to steric or electronic constraints. Depending on the energy barrier, some atropisomers interconvert rapidly, whereas others possess half-lives of years and can therefore be considered as configurationally stable. Like for other stereoisomers, opposite atropisomers often have markedly different properties, which can have important implications for drug development. An example is the muscarinic receptor antagonist telenzepine, which has two stable atropisomers of which one is 500-fold more active than the other.<sup>[1]</sup> In such cases, it is desirable to obtain atropisomers in an enantioenriched form. This is often achieved by chromatographic separation, which is inefficient and therefore unattractive at industrial scale.<sup>[2]</sup> For this reason, methods for atroposelective synthesis attract increasing attention from synthetic chemists.<sup>[3,4]</sup> At the same time, several critical limitations remain for atropisomer-selective small-molecule catalysis.

A particularly attractive strategy for atroposelective synthesis would be to make use of metathesis. Olefin metathesis is one of the most powerful methods for carbon-carbon bond formation in modern synthetic organic chemistry. It provides facile access to complex olefins from readily available alkenes and generates only unproblematic by-products.<sup>[5]</sup> For these reasons, it has revolutionized synthetic chemistry from the preparative to the industrial scale. A key challenge in the field is to develop catalysts for stereoselective metathesis. This has been achieved using catalysts bearing enantiopure ligands, most often based on molybdenum or ruthenium complexes.

Atroposelective metathesis has only recently been reported with stereodynamic trienes that undergo an atroposelective arene-forming reaction catalyzed by a chiral molybdenum catalyst.<sup>[6]</sup> This reaction was performed in organic solvents, as are most other reactions in organic chemistry. However, given the urgent need for green chemistry and to enable resource-efficient enzymatic cascade processes, it would be desirable to conduct such reactions in an aqueous environment.<sup>[7,8]</sup>

We hypothesized that atroposelective reactions in aqueous media could be realized by artificial metalloenzymes (ArMs). These hybrid catalysts combine the broad reaction scope of organometallic catalysis with the excellent catalytic properties and mild reaction conditions inherent to enzymatic catalysis.<sup>[9]</sup> ArMs result from the incorporation of an abiotic metal cofactor into a host protein, thus providing an enantiopure second coordination sphere, potentially enabling both activity and selectivity of the hybrid catalyst. This strategy has been used to create biocatalysts for a wide range of new-to-nature reactions, including olefin metathesis.<sup>[10–14]</sup>

Previously, we have created ArMs for ring-closing metathesis (RCM) by incorporating a biotinylated ruthenium cofactor into the homotetrameric bacterial protein streptavidin (Sav).<sup>[15]</sup> Relying on the high affinity of Sav for biotin ( $K_D$  approx.  $10^{-15}$  M), this allowed the construction of ArMs for various metathesis reactions, which we could subsequently optimize by means of protein engineering and directed evolution.<sup>[15,16]</sup> While the metathesis products in these cases were achiral, we hypothesized that the well-defined three-dimensional reaction environment provided by the Sav scaffold could provide interactions favoring a single diastereomeric transition state leading to an enantioenriched product.

While enzymes are known for the excellent stereocontrol they can exert on reactions and have been applied in the preparation of enantiopure biaryl compounds,<sup>[17,18]</sup> atroposelective metathesis has not been described for any natural or artificial enzyme. Here, we demonstrate that Sav-based ArMs can promote the formation of an enantioenriched binaphthelene derivative by RCM in aqueous media. This represents the first example of atroposelective olefin metathesis in water.

## Results and Discussion

### Development of a water-soluble metathesis substrate

Previous triene substrates that can undergo atroposelective metathesis to form binaphthelene compounds were activated by molybdenum catalysts in toluene.<sup>[6]</sup> While these substrates are insoluble in water, we hypothesized that adding a polar group on the side chain of the reactive triene moiety would yield a water-soluble compound (***E/Z*-1**) (Figure 1a). We anticipated that this would render the substrate amenable to aqueous metathesis, and that the release of the polar side chain would create less soluble binaphthalene **2**, potentially increasing the dissociation of the product from the ArM. This

reaction would generate two atropisomers, as the rotation of the two naphthalene moieties is hindered, lending configurational stability (Figure 1a).

We therefore introduced a quaternary ammonium group on one side chain of the substrate to increase its water solubility. The corresponding trifluoroacetate salt (**(E/Z)-1**) could be synthesized starting from compound **3**, which can be converted to dibenzylic alcohol **4** using a previously-reported building block strategy (Figure 1b).<sup>[6]</sup> Homoallylic diol **5** can then be synthesized according to an established oxidation-allylation sequence.<sup>[6]</sup> Finally, functional group interconversion on the side chain of **5** to amine **6** and further to the ammonium salt provides the desired product (**(E/Z)-1**). Gratifyingly, we obtained the desired substrate (**(E/Z)-1**) as a mixture of E and Z isomers, albeit with moderate yields. Nonetheless, we were pleased to observe that (**(E/Z)-1**) showed sufficient solubility in D<sub>2</sub>O (40 mmol·L<sup>-1</sup>, entirely soluble).

Next, we examined the reactivity of (**(E/Z)-1**) using **AquaMet**, a commercially available and water-soluble metathesis catalyst (Figure 1c). After incubating (**(E/Z)-1**) with **AquaMet** for 24 h at 37 °C, we observed the desired product in LCMS and isolated compound **2** by reversed-phase liquid chromatography (RPLC). While the reactivity consistently remained low in pure water, we could increase yields up to more than 10-fold using phosphate-buffered saline (PBS, Table S1). Nonetheless, the total turnover number (TON) remained below 2 under all tested conditions.

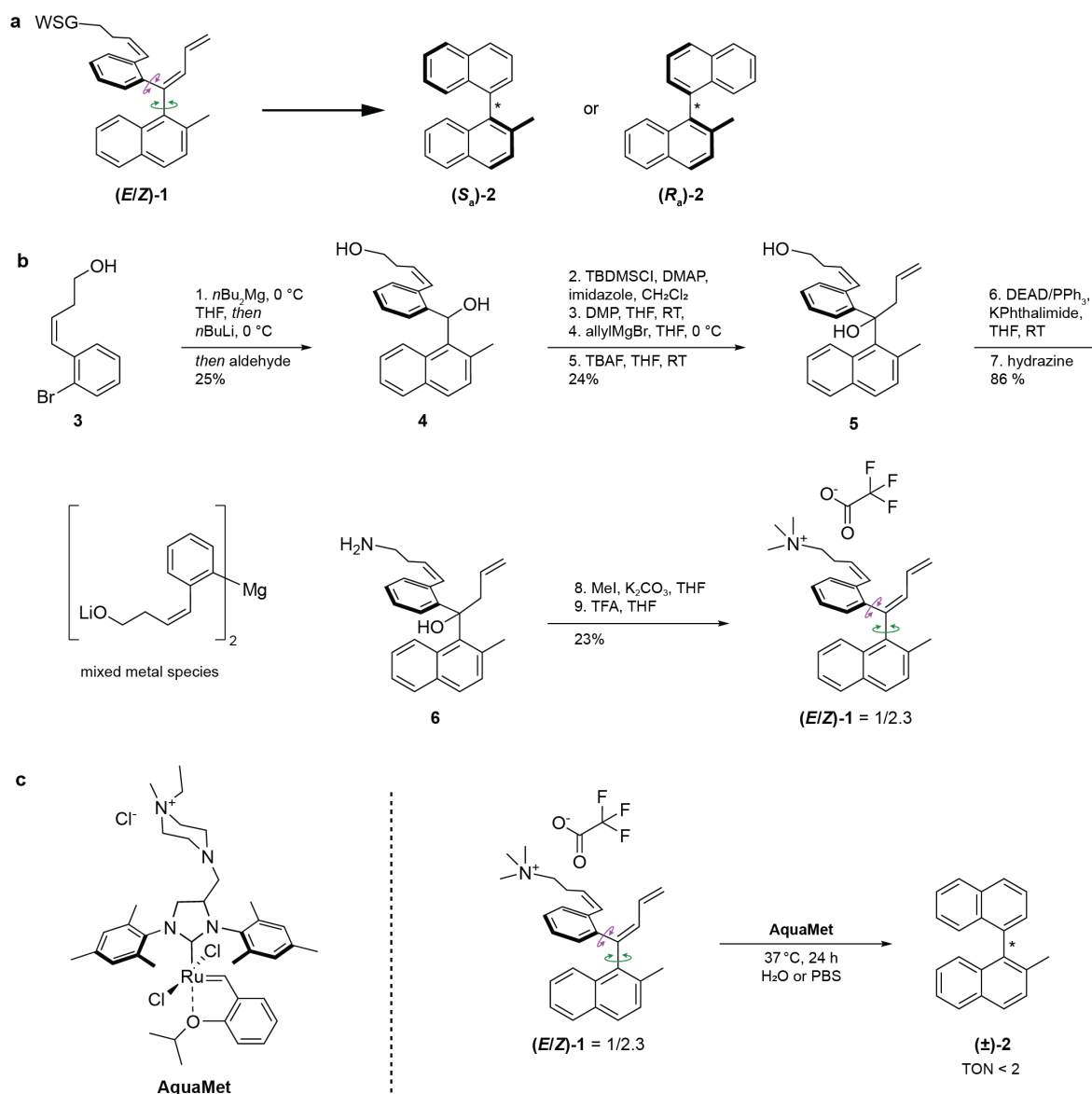


**Figure 1. A water-soluble substrate 1 for atroposelective metathesis.** (a) A water-soluble group (WSG) renders the triene substrate **(E/Z)-1** soluble in aqueous solution. Upon ring-closing metathesis (RCM), two atropisomers are produced, as the rotation around a single bond (\*) of the binaphthalene is hindered. (b) Synthetic route to the water-soluble substrate **(E/Z)-1** (see Methods). (c) The substrate **(E/Z)-1** undergoes RCM catalyzed by **AquaMet**. See Table S1 for details.

## ArMs enable atroposelective metathesis

With a water-soluble substrate and suitable analytics in hand, we investigated whether the reaction can be performed with a biotinylated Hoveyda-Grubbs catalyst (**Biot-NHC**)Ru, which we have used previously to construct ArMs (Figure 2a). While we did not observe conversion in pure water, the product was formed under various buffer conditions (Table S2). The best condition was PBS at a pH of 6.0 and 200 mM MgCl<sub>2</sub>, which gave comparably low TONs as observed for **AquaMet** (see above). Due to the low TONs, we performed subsequent screening experiments at a high catalyst loading of 73 % with respect to the reactive substrate isomer to ensure that we could analyze the enantiomeric ratio of the product. At this catalyst loading, we observed a yield of 43 % for free (**Biot-NHC**)Ru. As expected from the lack of possible chiral interactions with the small-molecule catalyst, the product was racemic (Figure 2b). Next, we sought to investigate whether the second coordination sphere provided by the Sav host protein could favor the formation of a single atropisomer. We had previously

engineered ArMs consisting of Sav and **(Biot-NHC)Ru** for RCM on a diallyl-sulfonamide substrate.<sup>[16]</sup> Relying on a bacterial whole-cell screening assay, we tested 400 Sav variants with substitutions at residues S112 and K121. These residues are in close proximity to the catalytic metal in Sav-based ArMs (Figure 2a) and have repeatedly been found to have a substantial impact on catalysis.<sup>[19,20]</sup> Based on these previous findings, we selected 23 Sav double mutants that are diverse in terms of amino acid properties at the residues 112 and 121, and had previously shown a high activity for RCM.<sup>[16]</sup> Next, we expressed and purified the selected Sav variants (Methods) and performed an *in vitro* activity assay with each mutant. Specifically, we assembled ArMs by incubating each variant with **(Biot-NHC)Ru**. Subsequently, we added **(E/Z)-1** and ran the reaction for 24 h at 37 °C. As depicted in Figure 2c, the protein scaffold had a pronounced influence on the yield of the RCM, which was highest (58 %) for the Sav mutant 112W 121V (abbreviated Sav WV), representing a modest improvement over the free catalyst (43 %). Notably, neither the free catalyst nor the ArMs achieved more than one turnover under our screening conditions (73 % catalyst loading).

Interestingly, Sav was able to induce atroposelectivity in the reaction, favoring either the  $S_a$ - or the  $R_a$ -isomer depending on the amino acids at positions 112 and 121. We observed the highest selectivity for the mutant containing two isoleucines (Sav II, 78:22 e.r.). The chromatogram displayed in Figure 2d illustrates how this ArM variant shifts the product composition compared to the free cofactor **(Biot-NHC)Ru**. Notably, three other mutants harboring branched, aliphatic amino acids induced a similar selectivity (Sav IV, LI and LV), whereas the IL, LL, VL, VI and VV mutants afforded moderate selectivity. This suggests that hydrophobic interactions might play a beneficial role during the reaction and that precise positioning of these interactions is crucial. Interestingly, two variants (Sav FT and Sav WT) led to an inversion of the selectivity, exhibiting a slight preference for the other enantiomer (43:57 and 34:66, respectively). Both mutants combine a bulky, hydrophobic amino acid in position 112 with a threonine at position 121. The latter appears to be crucial for inverting the selectivity, as exchanging it for serine, another polar amino acid of similar size (compare variants Sav FS and Sav WS), or valine (compare variant Sav WV) favors the opposite enantiomer. Similarly, exchanging phenylalanine or tryptophan at position 112 for a smaller amino acid (compare variants Sav DT and Sav VT) resulted in the original selectivity. This highlights that epistatic interactions between the two positions play a crucial role in determining the outcome of the reaction.

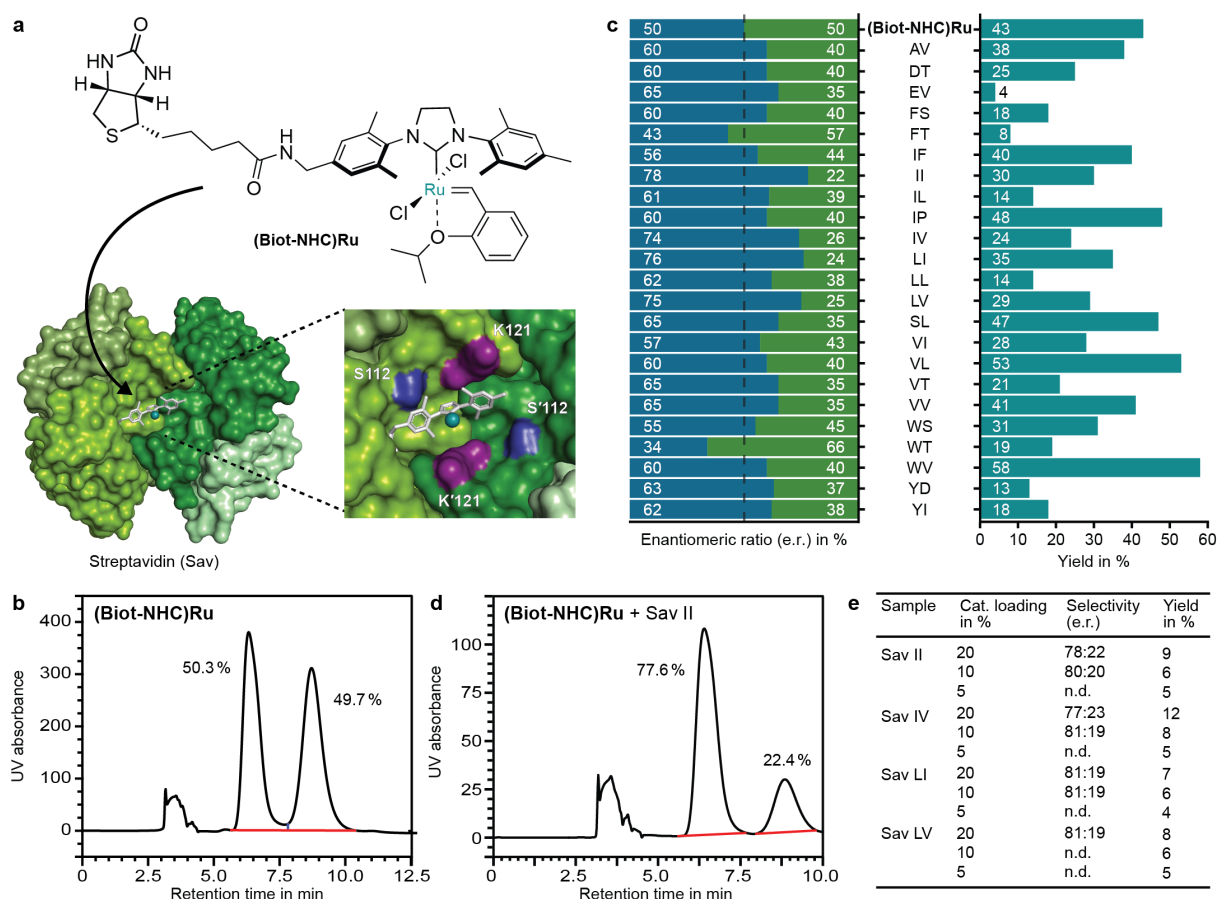


**Figure 2. Atroposelective metathesis catalyzed by artificial metalloenzymes.** (a) (Biot-NHC)Ru is anchored in streptavidin (Sav) to form an ArM. The residues S112 and K121 present in wild-type Sav are highlighted. X-ray crystal structure 5IRA from the Protein Data Bank. (b) HPLC analysis of the product resulting from the free cofactor (Biot-NHC)Ru. The two peaks correspond to the two atropisomers. The relative area of the two peaks is listed in the figure. Reactions were performed with 250  $\mu$ M (Biot-NHC)Ru and 344  $\mu$ M substrate (reactive isomer). The sample is identical to the one shown in panel c. (c) Summary of the screening of Sav S112X K121X double mutants. The two-letter code denotes the amino acids in positions 112 and 121. Reactions were performed with 500  $\mu$ M Sav biotin-binding sites, 250  $\mu$ M (Biot-NHC)Ru, and 344  $\mu$ M substrate (reactive isomer). (d) HPLC analysis of the product formed by an ArM consisting of (Biot-NHC)Ru and Sav 112I 121I (Sav II). The sample is identical to the one shown in panel c. (e) Reactions with the most selective mutants at catalyst loadings of 20 %, 10 % and 5 %. All reactions were performed with 344  $\mu$ M substrate and a 2:1 ratio of Sav biotin-binding sites to (Biot-NHC)Ru.

Having identified a number of promising ArMs for atroposelective metathesis, we tested various modifications to the reaction conditions to investigate whether the yield and selectivity can be increased further in this way. First, we investigated the performance of the four most selective mutants at lower catalyst loadings of 5, 10, and 20 %. Under these conditions, the ArMs displayed a similar enantiomeric ratio (up to 81:19), confirming the initially obtained results (Figure 2e). However, yields generally remained low regardless of the applied condition.

Moreover, we investigated the influence of the temperature (Table S3) and the ratio of Sav biotin-binding sites to catalyst (Table S4). Additionally, we tested whether the addition of co-solvents or crowding agents had a positive impact on the reaction sites (Table S5). However, none of these modifications led to noteworthy improvements in terms of yield or selectivity.

## Conclusion

Atroposelective metathesis catalyzed by ArMs in an aqueous environment represents an attractive addition to the synthetic chemistry and biocatalysis toolbox. The results presented in this study demonstrate the general feasibility of this concept and constitute a first step in this direction.

By embedding a biotinylated Hoveyda-Grubbs catalyst in Sav, it is possible to catalyze RCM on a triene substrate to form binaphthalene in an aqueous solution, albeit at modest yields and TONs. The latter remained low despite various modifications to the reaction conditions. This may be attributed to catalyst decomposition due to the unstable nature of Ru methyldene.<sup>[21,22]</sup> To overcome this challenge, one may envisage to rely on cyclic (alkyl)(amino)carbene ligands as these have been shown to increase the water stability of Ru-based metathesis catalysts significantly.<sup>[23]</sup>

Importantly, the second coordination sphere provided by the protein significantly influenced both the selectivity and the yield of the reaction. By engineering only two amino acid residues in the protein, we achieved a selectivity of up to 81:19 (e.r.). It also appears to be possible to access the opposite enantiomer, albeit with modest selectivity (up to 34:66 e.r.). Further improvements in selectivity and yield could potentially be achieved by engineering other positions in the protein or resorting to alternative ArM scaffolds that provide the possibility for intensified second-sphere interactions compared to the rather exposed biotin-binding vestibule in Sav. It is expected that stereoselective metathesis catalyzed by artificial metalloenzymes with high TONs and selectivities would enable the design of enzymatic cascade reactions to a diversity of medicinally relevant atropisomers.



## Methods

### Synthesis of the substrate (*E/Z*)-1

The synthesis was started by forming mixed metal species<sup>[24]</sup> after sequential treatment of **3** with *n*Bu<sub>2</sub>Mg, and lithium halogen exchange with *n*BuLi. After adding the mixed metal species to the aldehyde, diol **4** was isolated in a 25 % yield. The primary hydroxy group in the side chain was then silyl-protected using TBDMSCl, and the remaining secondary alcohol was oxidized to the ketone using DMP. The obtained ketone was then allylated using allyl-magnesium bromide. The TBDMS protecting group was removed with TBAF, giving homoallylic diol **5** in 24 % yield over four steps. Following a procedure for the Gabriel synthesis of amines under Mitsunobu conditions,<sup>[25]</sup> the selective substitution of the primary alcohol was achieved using potassium phthalimide. Mild deprotection using hydrazine hydrate was performed to obtain the desired aminoalcohol **6** in 86 % yield over two steps. The primary amine was alkylated using MeI to form a quaternary ammonium salt, and the tertiary alcohol was eliminated to form the reactive triene core. Finally, substrate (*E/Z*)-1 was obtained as a mixture of *E* and *Z* isomers in 23 % yield over two steps. Lower yields are presumably the consequence of a Hofmann elimination that takes place after quaternization in the presence of a base.

### Sav expression

A single colony of *E. coli* BL21-Gold(DE3) cells harboring a plasmid for periplasmic expression of the desired Sav variant was used to inoculate a starter culture (4 mL of LB with kanamycin (50 mg L<sup>-1</sup>)), which was grown overnight at 37 °C and 200 rpm. The expression plasmid contained a T7-tagged Sav gene with an N-terminal OmpA signal peptide for export to the periplasm under the control of the T7 promoter in a pET30b vector (Addgene #138589). On the following day, 100 mL of LB with kanamycin in a 500 mL flask was inoculated to an OD<sub>600</sub> of 0.01. The culture was grown at 37 °C and 200 rpm until it reached an OD<sub>600</sub> of 0.5. At this point, the flask was placed at room temperature for 20 min, and 50 μM IPTG was added to induce Sav expression. Expression was performed at 20 °C and 200 rpm overnight, and cells were harvested by centrifugation (3220 rcf, 4 °C, 15 min). Pellets were stored at -20 °C until purification.

### Sav purification

The cell pellets were resuspended in 10 mL lysis buffer (50 mM tris, 150 mM NaCl, 1 g L<sup>-1</sup> lysozyme, pH 7.4). After 30 min of incubation at room temperature, cell suspensions were subjected to three freeze-thaw cycles. Subsequently, nucleic acids were digested by addition of 10 μL of DNaseI (2000 units/mL, New England Biolabs) and CaCl<sub>2</sub> to a final concentration of 10 mM, followed by incubation at 37 °C for 45 min. After centrifugation, the supernatant was transferred to a new tube and mixed with 40 mL carbonate buffer (50 mM ammonium bicarbonate, 500 mM NaCl, pH 11). Pierce iminobiotin agarose (Thermo Fisher Scientific) was equilibrated in falcon tubes and used to pack a PD-10 column up to a bed height of approximately 1 cm. The lysate was loaded onto the column relying on gravity flow. Subsequently, the column was washed twice with 10 mL binding buffer. Eventually, Sav was eluted using 10 mL elution buffer (50 mM ammonium acetate and 500 mM NaCl, pH 4). Amicon Ultra filters (10 kDa molecular weight cut-off) were then used to concentrate the samples and exchange the buffer against PBS (200 mM MgCl<sub>2</sub>, pH 6).

## Quantification of biotin-binding sites

The concentration of Sav biotin-binding sites was determined using a modified version of the assay described by Kada et al.,<sup>[26]</sup> which relies on the quenching of the fluorescence of a biotinylated fluorophore upon binding to Sav. Specifically, 190  $\mu\text{L}$  of the binding site buffer (1  $\mu\text{M}$  biotin-4-fluorescein, 0.1  $\text{g L}^{-1}$  bovine serum albumin in PBS) was mixed with 10  $\mu\text{L}$  of Sav sample. After incubation at room temperature for 90 min, the fluorescence intensity was measured (excitation at 485 nm, emission at 525 nm), and a calibration curve produced with lyophilized Sav was used to calculate the concentration of Sav biotin-binding sites.

## *In vitro* catalysis

*In vitro* reactions were performed by mixing purified Sav, cofactor, substrate and buffer (PBS, 200 mM  $\text{MgCl}_2$ , pH 6) in a volume of 100  $\mu\text{L}$  or 200  $\mu\text{L}$  in glass vials. Concentrations varied between experiments and are given in the corresponding tables or figure captions. Reactions were carried out at 37  $^\circ\text{C}$  and 200 rpm for 24 h.

## Analytics

Samples were left at room temperature for 10 min, diluted in 1 mL acetonitrile and transferred to a 5 mL conical flask. Solvents were evaporated under reduced pressure. Subsequently, 50  $\mu\text{L}$  of a standard solution (1 mM 2-methoxynaphthalene in acetonitrile) and 50  $\mu\text{L}$  of acetonitrile were added, and the 100  $\mu\text{L}$  were injected into the RPLC for purification. The peak with a retention time of 15.56 min was collected. Solvents were evaporated and the product was dissolved in 100  $\mu\text{L}$  isopropanol. The samples were then injected into an HPLC using a chiral stationary phase (IJ column, heptane/isopropanol = 95/5) and two peaks corresponding to the two atropisomers were observed (retention time approximately 7 and 9 min).

## Author contributions

TV performed biological experiments and *in vitro* reactions. ZJ synthesized the substrate and performed analytics. VS performed preliminary experiments. MJ, CS, TRW and SP supervised the study. TV and MJ wrote the manuscript with input from all authors.

## Acknowledgments

This work was supported by the NCCR “Molecular Systems Engineering”, funded by the Swiss National Science Foundation.

## References

- [1] J. Clayden, W. J. Moran, P. J. Edwards, S. R. Laplante, *Angew. Chem. Int. Ed.* **2009**, *48*, 6398–6401.
- [2] S. T. Toenjes, J. L. Gustafson, *Future Med. Chem.* **2018**, *10*, 409–422.
- [3] B. Zilate, A. Castrogiovanni, C. Sparr, *ACS Catal.* **2018**, *8*, 2981–2988.
- [4] J. K. Cheng, S. H. Xiang, S. Li, L. Ye, B. Tan, *Chem. Rev.* **2021**, *121*, 4805–4902.
- [5] A. H. Hoveyda, A. R. Zhugralin, *Nature* **2007**, *450*, 243–251.
- [6] Z. Jončev, C. Sparr, *Angew. Chem. Int. Ed.* **2022**, *61*, e202211168.
- [7] D. K. Romney, F. H. Arnold, B. H. Lipshutz, C.-J. Li, *J. Org. Chem.* **2018**, *83*, 7319–7322.
- [8] V. Sabatino, T. R. Ward, *Beilstein J. Org. Chem.* **2019**, *15*, 445–468.
- [9] T. Vornholt, M. Jeschek, *ChemBioChem* **2020**, *21*, 2241–2249.
- [10] D. F. Sauer, S. Gotzen, J. Okuda, *Org. Biomol. Chem.* **2016**, *14*, 9174–9183.
- [11] A. R. Grimm, D. F. Sauer, M. D. Davari, L. Zhu, M. Bocola, S. Kato, A. Onoda, T. Hayashi, J. Okuda, U. Schwaneberg, *ACS Catal.* **2018**, *8*, 3358–3364.
- [12] T. Matsuo, C. Imai, T. Yoshida, T. Saito, T. Hayashi, S. Hirota, *Chem. Commun.* **2012**, *48*, 1662–1664.
- [13] C. Mayer, D. G. Gillingham, T. R. Ward, D. Hilvert, *Chem. Commun.* **2011**, *47*, 12068–12070.
- [14] M. Basauri-Molina, D. G. A. Verhoeven, A. J. Van Schaik, H. Kleijn, R. J. M. Klein Gebbink, *Chem. - Eur. J.* **2015**, *21*, 15676–15685.
- [15] M. Jeschek, R. Reuter, T. Heinisch, C. Trindler, J. Klehr, S. Panke, T. R. Ward, *Nature* **2016**, *537*, 661–665.
- [16] T. Vornholt, F. Christoffel, M. M. Pellizzoni, S. Panke, T. R. Ward, M. Jeschek, *Sci. Adv.* **2021**, *7*, eabe4208.
- [17] O. F. B. Watts, J. Berreur, B. S. L. Collins, J. Clayden, *Acc. Chem. Res.* **2022**, *55*, 3362–3375.
- [18] B. Skrobo, J. D. Rolfes, J. Deska, *Tetrahedron* **2016**, *72*, 1257–1275.
- [19] T. K. Hyster, L. Knorr, T. R. Ward, T. Rovis, *Science* **2012**, *338*, 500–503.
- [20] T. Heinisch, F. Schwizer, B. Garabedian, E. Csibra, M. Jeschek, J. Vallapurackal, V. B. Pinheiro, P. Marlière, S. Panke, T. R. Ward, *Chem. Sci.* **2018**, *9*, 5383–5388.
- [21] P. Schwab, R. H. Grubbs, J. W. Ziller, *J. Am. Chem. Soc.* **1996**, *118*, 100–108.
- [22] S. H. Hong, M. W. Day, R. H. Grubbs, *J. Am. Chem. Soc.* **2004**, *126*, 7414–7415.
- [23] C. O. Blanco, D. E. Fogg, *ACS Catal.* **2023**, *13*, 1097–1102.

- [24] D. Lotter, M. Neuburger, M. Rickhaus, D. Häussinger, C. Sparr, *Angew. Chem. Int. Ed.* **2016**, *55*, 2920–2923.
- [25] S. E. Sen, S. L. Roach, *Synthesis* **1995**, *1995*, 756–758.
- [26] G. Kada, K. Kaiser, H. Falk, H. J. Gruber, *Biochim. Biophys. Acta* **1999**, *1427*, 44–8.